# Approaching the Heisenberg Limit without Single-Particle Detection

Emily Davis, Gregory Bentsen, and Monika Schleier-Smith

Phys. Rev. Lett. **116**, 053601 — Published 2 February 2016

DOI: 10.1103/PhysRevLett.116.053601

# Approaching the Heisenberg limit without single-particle detection

Emily Davis, Gregory Bentsen, and Monika Schleier-Smith
*Department of Physics, Stanford University, Stanford, California 94305, USA*
(Dated: January 11, 2016)

We propose an approach to quantum phase estimation that can attain precision near the Heisenberg limit without requiring single-particle-resolved state detection. We show that the "one-axis twisting" interaction, well known for generating spin squeezing in atomic ensembles, can also amplify the output signal of an entanglement-enhanced interferometer to facilitate readout. Applying this interaction-based readout to oversqueezed, non-Gaussian states yields a Heisenberg scaling in phase sensitivity, which persists in the presence of detection noise as large as the quantum projection noise of an unentangled ensemble. Even in dissipative implementations—e.g., employing light-mediated interactions in an optical cavity or Rydberg dressing—the method significantly relaxes the detection resolution required for spectroscopy beyond the standard quantum limit.

For decades, advances in atomic spectroscopy have brought clocks, accelerometers, and magnetometers to ever greater precision. A recent development is the use of many-particle entangled states to reduce the statistical uncertainty in measurements of the energy difference $\hbar\omega$ between two atomic states $|\uparrow\rangle, |\downarrow\rangle$ [1–10]. Whereas an uncorrelated ensemble of $N$ two-level atoms achieves at best the standard quantum limit of precision $\Delta\omega T = 1/\sqrt{N}$ in an interrogation time $T$, entanglement can enhance this precision up to the fundamental Heisenberg limit $\Delta\omega T = 1/N$. Approaching the Heisenberg limit with more than a few particles remains a major outstanding challenge, due to difficulties not only of preparing but also of detecting entangled quantum states [11–13].

Imperfect state detection has limited the sensitivity of entanglement-enhanced metrology with squeezed [1–8], oversqueezed [9], and twin Fock [10] states. The standard detection protocol is to measure the population difference $n \equiv n_\uparrow - n_\downarrow$ between the levels $|\uparrow\rangle, |\downarrow\rangle$ in the entangled state after perturbing it by an amount proportional to the frequency $\omega$, with $dn/d\omega = NT$. Any uncertainty $\Delta n$ in the population measurement limits the attainable spectroscopic sensitivity to $\Delta\omega T > \Delta n/N$. Correspondingly, approaching the Heisenberg limit requires single-particle-resolved state detection, which becomes increasingly difficult at large atom number. Recent experiments have made progress in addressing this challenge [11, 12], but not yet under the conditions required to generate highly entangled states.

Theoretically, a quantum-enhanced measurement does not require directly detecting the entangled sensor state. Several proposals instead envision echo protocols [14–16] in which a quantum system undergoes a unitary evolution $U$ into a non-classical state and, after subjecting this state to a perturbation, one attempts to reverse the evolution to the initial state by application of $U^\dagger$. This approach in principle permits Heisenberg-limited measurements with an ensemble of spin-1/2 particles (or, equivalently, two-level atoms) by detecting the state of a single ancilla spin [16].

In this Letter, we propose an echo protocol that enables spectroscopy near the Heisenberg limit with low-resolution state detection $\Delta n \sim \sqrt{N}$. To generate entanglement, our method employs the global Ising interactions of the "one-axis twisting" Hamiltonian [17], realizable with cold atoms [4, 5, 18–22], trapped ions [23–25] and solid-state nuclear spins [26]. Switching the sign of the interaction after subjecting the system to a weak perturbation amplifies the perturbation into a larger spin rotation that is easily detected. We analyze the performance including dissipation in two atomic implementations, employing interactions mediated either by light in an optical cavity [19, 21] or by Rydberg dressing [27]. In each case, the twisting echo enables precision far beyond the standard quantum limit with detection noise larger than the quantum noise of an unentangled state.

The one-axis twisting Hamiltonian $H_{\text{twist}} = \chi S_z^2$ describes internal-state-dependent interactions in a collection of $N$ two-level atoms, which we represent in terms of spin-1/2 operators $\mathbf{s}_i$ by a collective spin $\mathbf{S} = \sum_{i=1}^{N} \mathbf{s}_i$. The dynamical effect of $H_{\text{twist}}$ is to generate a spin precession about the $\hat{\mathbf{z}}$-axis at a rate proportional to $S_z$ (Fig. 1**a**-**b**). For spins initially polarized along $\hat{\mathbf{x}}$, the lowest-order effect of $H_{\text{twist}}$ is squeezing [17]. At longer interaction time, $H_{\text{twist}}$ produces non-Gaussian states, including oversqueezed states and ultimately a maximally entangled GHZ state at $\chi t = \pi/2$ [24]. While the GHZ state enables Heisenberg-limited measurements in few-particle systems with highly coherent interactions, we will show that the twisting echo protocol attains a Heisenberg scaling $\Delta\omega T \propto 1/N$ at significantly shorter evolution time.

The squeezed and oversqueezed states generated by $H_{\text{twist}}$ are highly sensitive to spin rotations $\mathcal{R}_y(\phi) = e^{-i\phi S_y}$ about the $\hat{\mathbf{y}}$ axis. Indicative of this sensitivity are the increased quantum fluctuations $\Delta S_y$ in Fig. 1**b**, which lower the quantum Cramér-Rao bound on the uncertainty $\Delta\phi \geq 1/(2\Delta S_y)$ [28]. We therefore present a protocol for measuring $\mathcal{R}_y(\phi)$, bearing in mind that a compound sequence $\mathcal{R}_y(\phi) = \mathcal{R}_x(-\pi/2)\mathcal{R}_z(\phi)\mathcal{R}_x(\pi/2)$ then allows for measuring a precession $\phi = \Delta\omega T$ about $\hat{\mathbf{z}}$, much as in Ramsey spectroscopy with squeezed states [1–5].

The twisting echo protocol is shown in Fig. 1, where we assume unitary dynamics. An ensemble is initialized in the coherent spin state (CSS) $|\hat{\mathbf{x}}\rangle$ satisfying $S_x|\hat{\mathbf{x}}\rangle = S|\hat{\mathbf{x}}\rangle$ (Fig. 1**a**). Applying $H_{\rm twist}(\chi) = \chi S_z^2$ for a time $t$ yields the entangled state $|\psi_e\rangle = U|\hat{\mathbf{x}}\rangle$, where $U = e^{-i\chi S_z^2 t}$ (Fig. 1**b**). To detect a rotation $|\psi_e\rangle \to \mathcal{R}_y(\phi)|\psi_e\rangle$ by a small angle $\phi$, we attempt to undo the twisting by applying $H_{\rm twist}(-\chi)$. For $\phi = 0$, the final state $U^\dagger \mathcal{R}_y(\phi) U|\hat{\mathbf{x}}\rangle$ is identical to the original CSS. However, a non-zero angle $\phi$ (Fig. 1**c**) biases the $S_z$-dependent spin precession to produce a large final value of $\langle S_y\rangle$ (Fig. 1**d**). Measuring $S_y$, by rotating the state and then detecting the population difference $n_\uparrow - n_\downarrow$, provides a sensitive estimate of $\phi$.

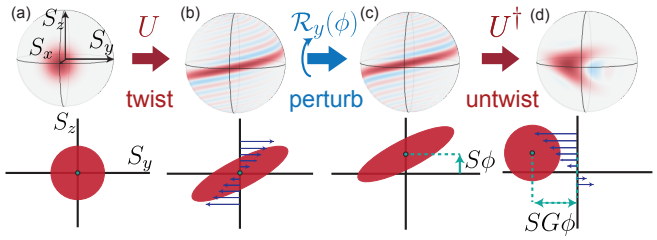


FIG. 1. **Twisting echo** for entanglement-enhanced measurement. Top row: The initial CSS $|\hat{\mathbf{x}}\rangle$ (**a**) evolves under $H_{\rm twist}(\chi)$ into an oversqueezed state $|\psi_e\rangle$ (**b**). To detect a rotation of $|\psi_e\rangle$ about $\hat{\mathbf{y}}$ by a small angle $\phi$ (**b**→**c**), we amplify the perturbation into a large displacement $\langle S_y^\phi\rangle = GS\phi$ by applying $H_{\rm twist}(-\chi)$ (**c**→**d**). Illustrated are Wigner quasiprobability distributions for $2S = 30$ atoms, with $\phi = 1/S$. Bottom row: Cartoon depiction of the same steps, with blue flow lines indicating twisting and untwisting.

The angular sensitivity is given by

$$\Delta\phi = \left[\Delta S_y^\phi / \partial_\phi \langle S_y^\phi\rangle\right]_{\phi=0}, \tag{1}$$

where $\langle S_y^\phi\rangle$ and $\Delta S_y^\phi$ represent the mean and standard deviation of $S_y$ after the echo, and $\partial_\phi \equiv d/d\phi$. The standard deviation for no rotation is ideally that of the initial CSS, $\Delta S_y^{\phi=0} = \Delta S_{\rm CSS} = \sqrt{S/2}$. To evaluate the denominator of Eq. 1, we expand

$$\begin{aligned}\langle S_y^\phi\rangle &= \langle\hat{\mathbf{x}}|U^\dagger e^{-i\phi S_y} U S_y U^\dagger e^{i\phi S_y} U|\hat{\mathbf{x}}\rangle \\ &= i\phi\langle\hat{\mathbf{x}}|[S_y, U^\dagger S_y U]|\hat{\mathbf{x}}\rangle + O(\phi^2).\end{aligned} \tag{2}$$

to lowest order in $\phi$. We express $S_y = (S_+ - S_-)/(2i)$ in terms of raising and lowering operators $S_\pm$ and simplify

$$U^\dagger S_\pm U = e^{-i\chi t S_z^2} S_\pm e^{i\chi t S_z^2} = S_\pm e^{i\chi t(\pm 2S_z + 1)} \tag{3}$$

to evaluate Eq. 2 using the generating functions in Ref. [29]. We thus arrive at a dependence

$$\left[\partial_\phi \langle S_y^\phi\rangle\right]_{\phi=0} = S(2S-1)\sin\left(\frac{Q}{2S}\right)\cos^{2S-2}\left(\frac{Q}{2S}\right) \tag{4}$$

of the final spin orientation on the perturbation $\phi$, where we have introduced the 'twisting strength' $Q \equiv 2S\chi t$. The resulting metrological gain $1/[N(\Delta\phi)^2]$ is plotted in Fig. 2**a** as a function of $Q$ for $N = 10^3$ atoms. At the optimal twisting strength $Q_{\rm opt} = 2S\,\mathrm{arccot}(\sqrt{2S-2}) \approx \sqrt{N}$ for $N \gg 1$, the echo protocol yields an angular sensitivity

$$\Delta\phi_{\rm min} = \sqrt{e}/N. \tag{5}$$

This sensitivity is very near the Heisenberg limit, despite a $\sim\sqrt{N}$-times shorter twisting evolution $Q_{\rm opt}$ than required to reach a GHZ state ($Q_{\rm GHZ}$ in Fig. 2**a**). The entangled state $|\psi_e\rangle$ at $Q_{\rm opt}$ is oversqueezed (Fig. 1**b**), allowing the echo to surpass the sensitivity $\Delta\phi \propto 1/N^{5/6}$ attainable by spin squeezing [17] under $H_{\rm twist}$.

The twisting echo is highly robust against detection noise (Fig. 2**b**), as the "untwisting" amplifies the spin rotation signal by a factor of $G \equiv d\langle S_y^\phi\rangle/d(S\phi) \le \sqrt{N}$ (Fig. 1**c**-**d**). Concomitantly, the quantum noise returns to the CSS level, so that adding Gaussian detection noise $\Delta S_{\rm meas} = \rho\Delta S_{\rm CSS}$ results in an angular sensitivity $\Delta\phi = \sqrt{1+\rho^2}\Delta\phi_{\rm min}$. Thus, even a measurement that barely resolves a CSS, with atom number resolution $\Delta n = 2\Delta S_{\rm meas} \approx \sqrt{N}$, permits a sensitivity near the Heisenberg limit. By contrast, measurement noise significantly degrades the sensitivity attainable by direct detection of non-Gaussian states: already at single-atom resolution, the twisting echo outperforms direct detection of a GHZ state (Fig. 2**b**).

In practice, the sensitivity $\Delta\phi$ may be degraded by imperfect coherence of the one-axis twisting evolution. To show that the twisting echo can provide a significant benefit in realistic metrological scenarios, we analyze the limitations due to dissipation in two implementations designed to enhance atomic clocks: the method of cavity feedback dynamics [19] demonstrated in Refs. [2, 20]; and the Rydberg dressing scheme proposed in Ref. [27].

*Cavity-Mediated Interactions* — The scheme for one-axis twisting by light-mediated interactions [19–21] is shown in Fig. 3**a**. Atoms in hyperfine states $|\uparrow\rangle, |\downarrow\rangle$ are coupled to an optical resonator mode with vacuum Rabi frequency $2g$, at large detunings $\pm\Delta$ from transitions to an excited state $|e\rangle$. The dispersive atom-light interaction shifts the cavity resonance frequency in proportion to $S_z$, with $\partial\omega_c/\partial S_z = \Phi\kappa/2$, where $\Phi \equiv 4g^2/\Delta\kappa$. Thus, driving the cavity at a detuning $\delta_C$ from the bare-cavity resonance results in an $S_z$-dependent intracavity power. The latter acts back on the atomic levels via the a.c. Stark shift, yielding an $S_z$-dependent spin precession. For small cavity shifts $\sqrt{N}\Phi\kappa \ll \delta_C$, the spin precession rate depends linearly on $S_z$, yielding one-axis twisting dynamics. The sign of the twisting is controlled by $\delta_c$, while the strength depends on the average number of photons $p$ in the coherent field incident on the cavity: $Q = 2Sp\Phi^2 d/(1+d^2)^2$, where $d = 2\delta_C/\kappa$.

The light-induced twisting is accompanied by fluctuations in the phase of the collective spin due to photon shot noise. These fluctuations are described by a

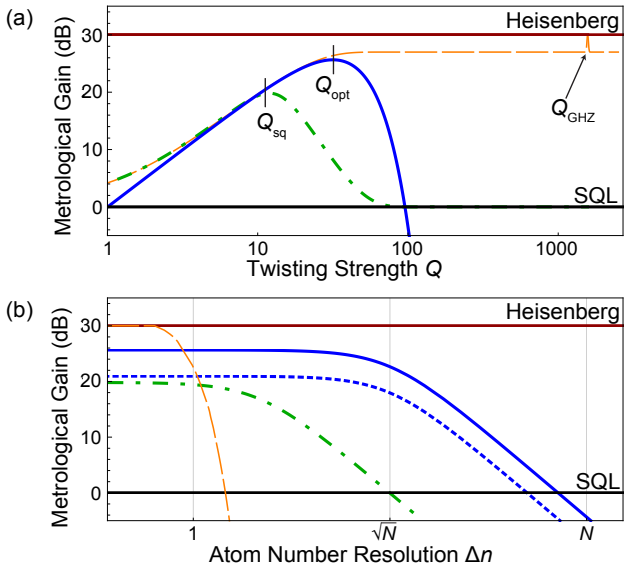


FIG. 2. **Metrological gain of the twisting echo** with $N = 10^3$ atoms. Horizontal lines indicate SQL (black) and Heisenberg limit (red). (**a**) Metrological gain *vs.* twisting strength $Q$ for the unitary twisting echo (solid blue), compared to spin squeezing (dot-dashed green) and the quantum Cramér-Rao bound (QCRB) on phase sensitivity (dashed orange). The twisting echo nearly follows the QCRB to its plateau at $Q \approx \sqrt{N}$; only at a much longer time $Q_{\rm GHZ} = N\pi/2$ does the QCRB increase by 3 dB to reach the Heisenberg limit. (**b**) Metrological gain *vs.* measurement uncertainty $\Delta n$ for echo with twisting strength $Q_{\rm opt}$ (solid blue) or $Q_{\rm sq}$ (dotted blue), compared to direct detection of the squeezed state at $Q_{\rm sq}$ (dot-dashed green). Dashed orange curve shows Cramér-Rao bound for estimating $\phi$ in the GHZ state $\mathcal{R}_y(\phi)(|\hat{\mathbf{y}}\rangle + |-\hat{\mathbf{y}}\rangle)$ using projective measurements with uncertainty $\Delta n$.

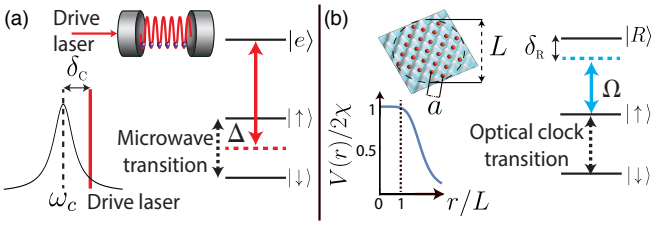


FIG. 3. **Experimental schemes** for entanglement-enhanced measurement. (**a**) Optical cavity with drive laser at detuning $\delta_C$ from cavity resonance $\omega_c$ and detunings $\pm\Delta$ from atomic transitions $|\uparrow\rangle \to |e\rangle$, $|\downarrow\rangle \to |e\rangle$. (**b**) Optical-lattice clock with metastable state $|\uparrow\rangle$ coupled to a Rydberg state $|R\rangle$ by a laser with Rabi frequency $\Omega$, producing the two-body potential $V(r)$ [27]. Both schemes yield one-axis twisting dynamics, with the sign of $H_{\rm twist}$ dictated by the sign of $\delta_C$ ($\delta_R$) in the cavity-QED (Rydberg) system.

Lindblad operator $L = \sqrt{\gamma}S_z$ in the master equation for the density matrix of the spin subsystem, where $\gamma = 2\chi/d$ [30]. Physically, $\gamma t$ represents the average number of photons rescattered into the cavity per atom while twisting. The leakage of these photons from the cavity in principle enables a measurement of $S_z$, whose backaction is the dephasing described by a decay in $\langle (S_\pm^{\phi=0})^2\rangle = e^{-4\gamma t}\langle (S_\pm^{t=0,\phi=0})^2\rangle$ after twisting and untwisting. Accordingly, to lowest order in $\gamma t \ll 1$, for $N \gg 1$, the variance of $S_y$ grows to

$$\left(\Delta S_y^{\phi=0}\right)^2 / {\Delta S_{\rm CSS}}^2 \approx 1 + 4S\gamma t = 1 + 4Q/d. \quad (6)$$

Thus, cavity decay increases $\Delta\phi$ by a factor $\sqrt{1+4Q/d}$ compared with the unitary case.

The phase broadening can be made arbitarily small at large detuning $\delta_C$ at the price of increased decoherence from spontaneous emission. The latter occurs at a rate $\Gamma_{\rm sc} = \chi(1/d + d)/(2\eta)$ per atom, where $\eta \equiv 4g^2/(\kappa\Gamma)$ is the single-atom cooperativity and $\Gamma$ is the excited-state linewidth. Assuming each spontaneous emission event has a probability $r$ of flipping a spin, the average value of $S_z$ while "untwisting" differs from that during "twisting" by a root-mean-square value [19] $\Delta S_z^{\rm sc} \approx \sqrt{4rS\Gamma_{\rm sc}t/3} = \sqrt{rQ(1/d+d)/(3\eta)}$. Such a change has the same effect on the final signal as a perturbation $\Delta\phi_{\rm sc} = \Delta S_z^{\rm sc}/S$, and thus contributes to the uncertainty in measuring $\phi$.

To calculate the phase sensitivity of the dissipative echo, we first express the normalized phase variance $\sigma_0^2 \equiv 2S\,(\Delta\phi)_0^2$ for the unitary case in terms of the twisting strength $Q$. From Eq. 4, using the approximation $\cos^{2S-2}(\chi t) \approx e^{-S(\chi t)^2}$ for $\chi t \ll 1$, we obtain $\sigma_0^2 \approx e^{Q^2/(2S)}/Q^2$. The total phase including cavity decay and spontaneous emission is then given by $\sigma^2 \equiv 2S\,(\Delta\phi)^2 = \sigma_0^2 + \sigma_{\rm diss}^2$, where

$$\sigma_{\rm diss}^2 = 4e^{Q^2/(2S)}/(Qd) + 2rQ\left(d^{-1} + d\right)/(3S\eta) \quad (7)$$

represents the noise added by dissipation. This noise will reduce the optimal twisting strength below $Q_{\rm opt} = \sqrt{2S}$, so that $e^{Q^2/(2S)} \sim 1$. The dissipative contribution $\sigma_{\rm diss}^2$ is then minimized by choosing $Qd \approx \sqrt{6S\eta/r}$ and large detuning $d \gg 1$, yielding a total variance

$$\sigma^2 \approx r(1+d^2)/(6S\eta) + \sqrt{32r(1+1/d^2)/(3S\eta)}. \quad (8)$$

At large collective cooperativity $2S\eta \gg 1$, the normalized phase variance $\sigma^2$ depends only weakly on detuning (Fig. 4**a**.i) for $1 \ll d \ll \sqrt[4]{S\eta/r}$, where we obtain $\sigma^2 \approx \sigma_{\rm diss}^2 \approx \sqrt{32r/(3S\eta)}$. We plot the metrological gain $\sigma^{-2}$ as a function of $N$ and $\eta$ in Fig. 4**a**.ii.

The scaling of the metrological gain with collective cooperativity is just as in spin squeezing by quantum non-demolition measurement [32], but no coherence-preserving measurement is required. Moreover, the measurement only requires a resolution on the order of the width $\Delta S_y^\phi \geq \Delta S_{\rm CSS}$ of the broadened final state. The benefits of the echo for state detection can be combined with schemes for reducing dissipation [13, 33, 34] to achieve even higher sensitivity.

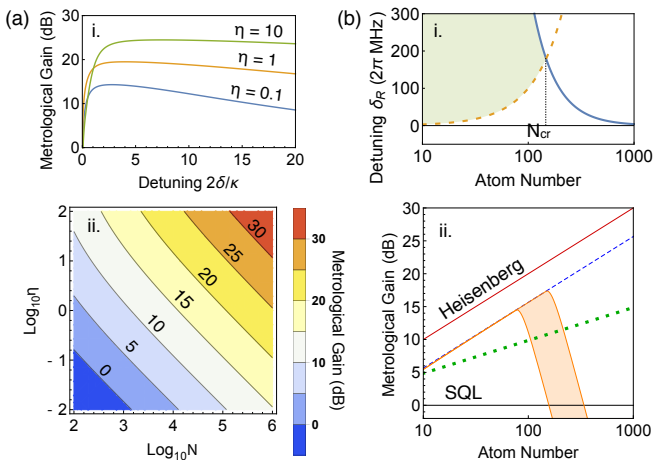


FIG. 4. **Dissipative twisting echo.** (**a**) Cavity-mediated twisting, with $r = 1/2$. (**i**) Metrological gain $-10\log_{10}\sigma^2$ *vs.* laser-cavity detuning $d = 2\delta_C/\kappa$ for $N = 10^5$ atoms and cooperativity $\eta = 0.1$ (blue), 1 (orange), 10 (green). (**ii**) Metrological gain *vs.* $N$ and $\eta$. (**b**) Rydberg-mediated twisting in Sr for $n = 70$, $2a = 800$ nm, $\epsilon = 0.1$. (**i**) Limitations on the detuning $\delta_R$, which must lie below the blue line for all atoms to fit inside the interaction sphere, but above the dotted orange line to avoid spontaneous emission. (**ii**) Metrological gain *vs.* $N$ in Rydberg scheme limited by spontaneous emission (orange), compared to idealized case without spontaneous emission (dashed blue) and cavity-mediated twisting with $\eta = 10$ (dotted green). Orange band represents a range of $\overline{C}_6$ coefficients $10^{10} \leq \overline{C}_6 \leq 10^{11}$ calculated for principal quantum numbers $60 \lesssim n \lesssim 70$ [31].

*Rydberg Dressing*—To approach the ideal unitary echo, we consider implementing $H_{\rm twist}$ by Rydberg dressing (Fig. 3**b**) in a strontium optical-lattice clock [27]. Here, the pseudo-spin states are the singlet ground state $|\downarrow\rangle = |^1S_0\rangle$ and metastable triplet state $|\uparrow\rangle = |^3P_0\rangle$. A laser with Rabi frequency $\Omega$ is detuned by $\delta_R$ from the $|\uparrow\rangle \rightarrow |R\rangle$ transition, where $|R\rangle = |n^3S_1\rangle$ represents a Rydberg state of principal quantum number $n$. The coupling to $|R\rangle$ induces a two-body potential $V(r)$ that is nearly constant over a distance $L = \frac{1}{2}[C_6/(2\delta_R)]^{1/6}$ (Fig. 3**b**), enabling all-to-all interactions among $N$ atoms confined within a region of diameter $L$. In the limit of weak dressing, where the probability $\epsilon \equiv N_\uparrow\Omega^2/(4\delta_R^2)$ for even a single one of the $N_\uparrow \approx N/2$ spin-up atoms to be excited to $|R\rangle$ is small ($\epsilon \ll 1$), the result is a one-axis twisting Hamiltonian with interaction strength $\chi = \Omega^4/(16\delta_R^3)$ [27]. The sign of the interaction is controlled by the detuning $\delta_R$, while the strength $|\chi| = \epsilon^2 C_6/(2^5N^2L^6)$ is highest for small, dense ensembles.

Obtaining maximally coherent all-to-all interactions requires careful choice of the detuning from the Rydberg state. The detuning $\delta_R$ controls both the interaction range $L$ and the ratio $\chi/\Gamma_{\rm sc} \propto \delta_R$ between the spin-spin coupling and the spontaneous emission rate $\Gamma_{\rm sc} = \epsilon\Gamma/N$ per atom, where $\Gamma$ is the Rydberg state linewidth. To fit all atoms inside a sphere of diameter $L$ in a three-dimensional lattice with spacing $a$, we must restrict the detuning to $\delta_R < \Gamma\overline{C}_6/(2^9N^2)$, where $\overline{C}_6 \equiv C_6/(\Gamma a^6)$. To conservatively estimate the metrological gain attainable under this restriction, without modeling the effects of decay to other Rydberg states, we restrict the twisting-untwisting evolution to the first spontaneous emission event: $2N\Gamma_{\rm sc}t \lesssim 1$. Reaching the optimum oversqueezed state at $Q_{\rm opt}$ then requires a detuning $\delta_R > \Gamma N^{3/2}/(2\epsilon)$. Both conditions on $\delta_R$, plotted in Fig. 4**b**.i, can be met simultaneously for up to $N_{\rm cr} = (\overline{C}_6\epsilon/2^8)^{2/7}$ atoms. Here, $\overline{C}_6 \sim 10^{11}$ for a Rydberg state of principal quantum number $n \sim 70$ [31] in a lattice of the "magic" wavelength $2a \approx 800$ nm for the clock transition [35]. At a Rydberg-state population $\epsilon = 0.1$, the ideal phase sensitivity of Eq. 5 can then be reached with up to $N_{\rm cr} \approx 150$ atoms.

We compare the predicted performance of the Rydberg and cavity schemes in Fig. 4**b**.ii. For low atom number, the Rydberg dressing outperforms cavity-mediated interactions even at strong coupling $\eta \sim 10$. Yet whereas the cavity echo improves monotonically with $N$, the Rydberg echo reaches an optimum at the critical atom number $N_{\rm cr}$, above which the coherent evolution time must be reduced to extend the interaction range. Even with only $N_{\rm cr} \approx 150$ atoms, the twisting echo matches the phase sensitivity of $\sim 10^4$ unentangled atoms. The method could thus benefit atomic clocks employing asynchronous interrogation of many small sub-ensembles [36, 37].

We have presented a protocol that amplifies the effect of a phase rotation on an entangled state to enhance signal readout. By transferring the phase information to the average displacement of a near-Gaussian state, the twisting echo attains a Heisenberg scaling in sensitivity without single-particle resolution, and eliminates the need for Bayesian estimation methods for non-Gaussian states. Our approach can guide the design of new experiments by alleviating the need to simultaneously optimize coherence of interactions and fidelity of state detection. The protocol is adaptable to a wide range of systems, including ones where the sign of the interaction is fixed. For example, spin rotations can convert one-axis twisting to a two-axis counter-twisting Hamiltonian $H_{\rm ct} \propto S_x^2 - S_y^2$ [38] and can switch the sign of $H_{\rm ct}$ to exchange the squeezed and amplified quadratures. Future work might explore extensions to richer many-body systems featuring finite-range interactions or chaotic dynamics.

This work was supported by the AFOSR, the Alfred P. Sloan Foundation, the NSF, and the Fannie and John Hertz Foundation. We thank V. Vuletić, A. S. Sørensen, M. Kasevich, and O. Hosten for helpful discussions.

[1] V. Meyer, M. A. Rowe, D. Kielpinski, C. A. Sackett, W. M. Itano, C. Monroe, and D. J. Wineland, Phys.

Rev. Lett. **86**, 5870 (2001).
[2] I. D. Leroux, M. H. Schleier-Smith, and V. Vuletić, Phys. Rev. Lett. **104**, 250801 (2010).
[3] A. Louchet-Chauvet, J. Appel, J. J. Renema, D. Oblak, N. Kjaergaard, and E. S. Polzik, New J. of Phys. **12**, 065032 (2010).
[4] C. Gross, T. Zibold, E. Nicklas, J. Estéve, and M. K. Oberthaler, Nature **464**, 1165 (2010).
[5] C. F. Ockeloen, R. Schmied, M. F. Riedel, and P. Treutlein, Phys. Rev. Lett. **111**, 143001 (2013).
[6] R. J. Sewell, M. Koschorreck, M. Napolitano, B. Dubost, N. Behbood, and M. W. Mitchell, Phys. Rev. Lett. **109**, 253605 (2012).
[7] C. D. Hamley, C. S. Gerving, T. M. Hoang, E. M. Bookjans, and M. S. Chapman, Nat Phys **8**, 305 (2012).
[8] T. Berrada, S. van Frank, R. Bücker, T. Schumm, J. F. Schaff, and J. Schmiedmayer, Nat Commun **4** (2013).
[9] H. Strobel, W. Muessel, D. Linnemann, T. Zibold, D. B. Hume, L. Pezzé, A. Smerzi, and M. K. Oberthaler, Science **345**, 424 (2014).
[10] B. Lücke, M. Scherer, J. Kruse, L. Pezzé, F. Deuretzbacher, P. Hyllus, O. Topic, J. Peise, W. Ertmer, J. Arlt, L. Santos, A. Smerzi, and C. Klempt, Science **334**, 773 (2011).
[11] H. Zhang, R. McConnell, S. Ćuk, Q. Lin, M. H. Schleier-Smith, I. D. Leroux, and V. Vuletić, Phys. Rev. Lett. **109**, 133603 (2012).
[12] D. Hume, I. Stroescu, M. Joos, W. Muessel, H. Strobel, and M. Oberthaler, Phys. Rev. Lett. **111**, 253001 (2013).
[13] J. Bohnet, K. Cox, M. Norcia, J. Weiner, Z. Chen, and J. Thompson, Nature Photonics **8**, 731 (2014).
[14] B. Yurke, S. L. McCall, and J. R. Klauder, Phys. Rev. A **33**, 4033 (1986).
[15] F. Toscano, D. A. R. Dalvit, L. Davidovich, and W. H. Zurek, Phys. Rev. A **73**, 023803 (2006).
[16] G. Goldstein, P. Cappellaro, J. R. Maze, J. S. Hodges, L. Jiang, A. S. Sørensen, and M. D. Lukin, Phys. Rev. Lett. **106**, 140502 (2011).
[17] M. Kitagawa and M. Ueda, Phys. Rev. A **47**, 5138 (1993).
[18] A. Sørensen, L. M. Duan, J. I. Cirac, and P. Zoller, Nature **409**, 63 (2001).
[19] M. H. Schleier-Smith, I. D. Leroux, and V. Vuletić, Phys. Rev. A **81**, 021804 (2010).
[20] I. D. Leroux, M. H. Schleier-Smith, and V. Vuletić, Phys. Rev. Lett. **104**, 073602 (2010).
[21] Y.-L. Zhang, C.-L. Zou, X.-B. Zou, L. Jiang, and G.-C. Guo, Phys. Rev. A **91**, 033625 (2015).
[22] A. S. Sørensen and K. Mølmer, Phys. Rev. A **66**, 022314 (2002).
[23] A. Sørensen and K. Mølmer, Phys. Rev. Lett. **82**, 1971 (1999).
[24] T. Monz, P. Schindler, J. T. Barreiro, M. Chwalla, D. Nigg, W. A. Coish, M. Harlander, W. Hänsel, M. Hennrich, and R. Blatt, Phys. Rev. Lett. **106**, 130506 (2011).
[25] J. W. Britton, B. C. Sawyer, A. C. Keith, C. C. J. Wang, J. K. Freericks, H. Uys, M. J. Biercuk, and J. J. Bollinger, Nature **484**, 489 (2012).
[26] M. Rudner, L. Vandersypen, V. Vuletić, and L. Levitov, Phys. Rev. Lett. **107**, 206806 (2011).
[27] L. I. R. Gil, R. Mukherjee, E. M. Bridge, M. P. A. Jones, and T. Pohl, Phys. Rev. Lett. **112**, 103601 (2014).
[28] V. Giovannetti, S. Lloyd, and L. Maccone, Nat Photon **5**, 222 (2011).
[29] F. T. Arecchi, E. Courtens, R. Gilmore, and H. Thomas, Phys. Rev. A **6**, 2211 (1972).
[30] See Supplemental Material [url], which includes Ref. [39].
[31] C. L. Vaillant, M. P. A. Jones, and R. M. Potvliege, J. Phys. B **45**, 135004 (2012); S. Kunze, R. Hohmann, H.-J. Kluge, J. Lantzsch, L. Monz, J. Stenner, K. Stratmann, K. Wendt, and K. Zimmer, Z. Phys. D **27**, 111 (1993).
[32] K. Hammerer, K. Mølmer, E. S. Polzik, and J. I. Cirac, Phys. Rev. A **70**, 044304 (2004).
[33] M. Saffman, D. Oblak, J. Appel, and E. S. Polzik, Phys. Rev. A **79** (2009).
[34] C. M. Trail, P. S. Jessen, and I. H. Deutsch, Phys. Rev. Lett. **105**, 193602 (2010); I. D. Leroux, M. H. Schleier-Smith, H. Zhang, and V. Vuletić, Phys. Rev. A **85**, 013803 (2012).
[35] J. Ye, H. J. Kimble, and H. Katori, Science **320**, 1734 (2008); H. Katori, Nature Photonics **5** (2011).
[36] G. Biedermann, K. Takase, X. Wu, L. Deslauriers, S. Roy, and M. Kasevich, Phys. Rev. Lett. **111**, 170802 (2013).
[37] J. Borregaard and A. S. Sørensen, Phys. Rev. Lett. **111**, 090802 (2013).
[38] Y. C. Liu, Z. F. Xu, G. R. Jin, and L. You, Phys. Rev. Lett. **107**, 013601 (2011).
[39] F. Reiter and A. S. Sørensen, Phys. Rev. A **85**, 032111 (2012).